

One-Step Synthesis of AuCu/TiO₂ Catalysts for CO Preferential Oxidation

Catarine Santos Lopes Alencar^a, Ana Rita Noborikawa Paiva^a, Julio Cesar Martins da Silva^{a,b},

Jorge Moreira Vaz^a, Estevam Vitorio Spinacé^{a*} 

^aInstituto de Pesquisas Energéticas e Nucleares (IPEN-CNEN/SP), Av. Prof. Lineu Prestes, 2242, Cidade Universitária, 05508-900, São Paulo, SP, Brasil

^bUniversidade Federal Fluminense, Instituto de Química, Outeiro de São João Batista, s/n, Campus do Valonguinho, Centro, 24020-141, Niterói, RJ, Brasil

Received: April 29, 2020; Revised: September 17, 2020; Accepted: September 27, 2020

Au/TiO₂ (1wt% Au), Cu/TiO₂ (1wt% Cu) and AuCu/TiO₂ (1wt% AuCu) catalysts with different Au:Cu mass ratios were prepared in one-step synthesis using sodium borohydride as reducing agent. The resulting catalysts were characterized by X-ray diffraction (XRD), X-ray Dispersive Energy (EDX), Transmission Electron Microscopy (TEM) and Temperature Programmed Reduction (TPR) and tested for the preferential oxidation of carbon monoxide (CO-PROX reaction) in H₂-rich gases. EDS analysis showed that the Au contents are close to the nominal values whereas for Cu these values are always lower. X-ray diffractograms showed only the peaks of TiO₂ phase; no peaks of metallic Au and Cu species or oxides phases were observed. TPR and high-resolution TEM analysis showed that AuCu/TiO₂ catalysts exhibited most of Au in the metallic form with particles sizes in the range of 3-5 nm and that Cu was found in the form of oxide in close contact with the Au nanoparticles and well spread over the TiO₂ surface. The AuCu/TiO₂ catalysts exhibited good performance in the range of 75-100 °C and presented a better catalytic activity when compared to the monometallic ones. A maximum CO conversion of 98.4% with a CO₂ selectivity of 47% was obtained for Au_{0.50}Cu_{0.50}/TiO₂ catalyst at 100°C.

Keywords: AuCu/TiO₂ catalyst, carbon monoxide, preferential oxidation, hydrogen.

1. Introduction

Hydrogen gas is produced predominantly by combining the methane steam reforming and the gas-water shift reactions resulting in a hydrogen-rich mixture containing about 1% of carbon monoxide (10.000 ppm of CO). This CO level is not sufficiently low for application of hydrogen in Proton Exchange Membrane Fuel Cell (PEMFC) and in ammonia synthesis because CO poisons the catalysts used in these processes¹⁻⁵. Therefore, the purification of the hydrogen-rich mixture is necessary and one process that has been considered very promising is the preferential oxidation of CO in hydrogen-rich mixtures (CO-PROX reaction), because it can dramatically reduce energy and hydrogen losses when compared to the processes currently used in the industry such as CO methanation and pressure swing adsorption (PSA). However, the catalysts for CO-PROX reaction should be active and especially highly selective, as it should selectively oxidize CO and avoid hydrogen oxidation¹⁻⁵.

Au nanoparticles supported on TiO₂ (Au/TiO₂ catalyst) showed good CO conversions and CO₂ selectivity for CO-PROX reaction in the range of 20 to 100°C; however, the procedure used to prepare Au/TiO₂ catalysts has a significant influence on the catalytic performance, which is a result of Au nanoparticles sizes (should be smaller than 5 nm) and

Au-TiO₂ interactions⁶⁻¹². Sangeetha et al.¹³ prepared Au nanoparticles supported on CuO_x-TiO₂ (x from 1 and 10 wt%), where the support was prepared by impregnation of Cu(NO₃)₂ in TiO₂ (Degussa P25) and treating at 350°C. The deposition of Au nanoparticles was carried out by the deposition-precipitation method obtaining nanoparticle sizes of about 2.5 nm. The resulting Au/CuO_x-TiO₂ catalysts were more active than the Au/TiO₂ catalyst with CO conversions close to 100% and CO₂ selectivity values of 60 to 80% in the temperature range of 50 °C to 100 °C. Duh et al.¹⁴ also prepared a series of Au/CuO_x-TiO₂ catalysts with various Cu/Ti ratios by incipient-wetness impregnation and Au was supported by deposition-precipitation. It was observed that the addition of CuO_x in Au/TiO₂ catalyst enhanced the activity significantly for CO oxidation at low temperature, which was attributed to the interactions among Au, CuO_x and TiO₂. Recently, Qi et al.¹⁵ prepared nanosized CuO and Cu₂O materials and followed by the deposition of Au nanoparticles. The catalytic activities of the resulting AuCu catalysts for CO-PROX showed a significant enhancement when compared to CuO and Cu₂O materials. It was concluded that CuO not Cu₂O species play a critical role for the CO oxidation and that the cooperative effect between CuO and Au nanoparticles enhanced the activity of Au/CuO catalyst when a strong interaction between them occurred.

*e-mail: espinace@ipen.br

In this work we prepare Au/TiO₂, Cu/TiO₂ and AuCu/TiO₂ catalysts in one-step synthesis by co-reducing the Au⁺³ and Cu⁺² ions with sodium borohydride in the presence of the TiO₂ support. The catalysts were characterized and tested for CO-PROX reaction.

2. Experimental

2.1 Synthesis of Au/TiO₂ catalyst (1.0 wt% Au)

A suspension containing 346.5 mg of TiO₂ (P25 Evonik) and 45 mL of deionized water was prepared. Then 6.12 x 10⁻⁴ L of tetrachlorouric acid (HAuCl₄) solution (2.88 x 10⁻² mol L⁻¹) was added and stirred for homogenization for about 10 min. After this, 2.02 x 10⁻⁴ L of NaBH₄ solution (2.643 x 10⁻¹ mol L⁻¹) was added and the resulting mixture remained under stirring for 24h. Then, the solid was then separated by centrifugation, washed with excess water and dried at 70 °C.

2.2 Synthesis of Cu/TiO₂ catalyst (1.0 wt% Cu)

The procedure was similar to that described above, but using 5.50 x 10⁻⁴ L of Cu(NO₃)₂ solution (1 x 10⁻¹ mol L⁻¹).

2.3 Synthesis of AuCu/TiO₂ catalyst with different mass ratios

The procedure was similar to that described above but using HAuCl₄ solution (2.88 x 10⁻² mol L⁻¹) and Cu(NO₃)₂ solution (1 x 10⁻¹ mol L⁻¹) in the desired proportions and 5.14 x 10⁻⁴ L of NaBH₄ solution (2.643 x 10⁻¹ mol L⁻¹). The pH of the synthesis solutions were in the range of 4.5 and 5.

2.4 Characterizations

The semi-quantitative chemical analysis of the catalysts were performed by Energy-dispersive X-ray spectroscopy (EDS) on a Philips Scanning Microscope model XL30 with 20 kV electron beam equipped with an EDAX model DX-4 micro analyzer.

Transmission electron microscopy (TEM) was performed on a JEOL Transmission Electron Microscope, model JEM-2100 (200 kV). The particle size distributions were obtained by measuring de diameter of more than 100 nanoparticles from the micrographs.

X-ray diffraction (XRD) was performed on a Rigaku Multiflex diffractometer using Cu K α radiation source ($\lambda = 1.5418\text{\AA}$) with 2 θ scan between 20° and 90°, with 0.06° step and time per step of 4s.

Temperature Programmed Reduction (TPR) experiments were performed on Quantachrome ChemBET Pulsar using 50 mg of catalyst in a U-shaped quartz cell and H₂ consumption was measured using a thermal conductivity detector (TCD). Initially the catalyst was treated in a flow of N₂ (50 mL min⁻¹) at 200 °C for 1 h and after cooling to room temperature the catalyst was exposed to gas containing 10% vol H₂/N₂ at a flow rate of 30 mL min⁻¹ and heated to 750°C at 10°C min⁻¹.

2.5 Catalytic tests

The catalytic tests were performed in a fixed bed reactor (U-tube) using 100 mg of catalysts in the temperature range between 25 °C to 150 °C using a gas composition containing 1 mol% of CO, 1mol% of O₂ and 98 mol% of H₂ (O₂/CO volumetric ratio of 1, $\lambda = 2$) and a flow rate of 25 mL min⁻¹ (spatial velocity of 15000 mL gcat⁻¹ h⁻¹). The reaction products and unconverted reagents were quantified using a Gas Chromatograph Agilent HP 7890A with TCD and FID (methanation of CO and CO₂) detectors. To evaluate the performance of each catalyst, CO conversion and CO₂ selectivity were calculated according to the Equations 1 and 2:

$$\text{CO conversion} = \frac{([\text{CO}_i] - [\text{CO}_f]) \times 100}{[\text{CO}_i]} \quad (1)$$

$$\text{CO}_2 \text{selectivity} = \frac{0.5 \times [\text{CO}_2 f] \times 100}{([\text{O}_2 i] - [\text{O}_2 f])} \quad (2)$$

3. Results and Discussion

The semi-quantitative EDS analyses of the catalysts are shown in Table 1.

In a general manner, it was observed that the amounts of Au and Cu determined by EDS increase with the increase of the nominal values; however, the values determined for Au are close to the nominal values, while for Cu these values are always smaller than the nominal ones. This could be explained by the EDS analysis having been performed in a semi-quantitative way and/or that not all Cu species were deposited on the TiO₂ support as the mother liquor was slightly colored after centrifugation.

The X-ray diffractograms of the TiO₂ support and Au/TiO₂, Cu/TiO₂ and Au_{0.50}Cu_{0.50}/TiO₂ catalysts are shown in Figure 1.

For all catalysts it was observed the diffraction peaks of the support TiO₂ P25, which has about 80% of anatase phase with 2 θ : 25.36°, 37.89°, 48.14°, 54.03°, 55.18° corresponding to the planes (101), (004), (200), (105),

Table 1. Chemical composition and average particle sizes of the catalysts.

Catalyst composition (wt%)	Au (wt%) EDS	Cu (wt%) EDS	d (nm) TEM
Au _{1.0} /TiO ₂	0.99	--	4.9 ± 1.2
Cu _{1.0} /TiO ₂	--	0.35	--
Au _{1.0} Cu _{0.90} /TiO ₂	0.10	0.45	3.5 ± 0.7
Au _{0.25} Cu _{0.75} /TiO ₂	0.31	0.29	3.6 ± 0.9
Au _{0.50} Cu _{0.50} /TiO ₂	0.73	0.25	2.9 ± 0.7
Au _{0.75} Cu _{0.25} /TiO ₂	0.87	0.21	3.9 ± 1.0
Au _{0.9} Cu _{0.1} /TiO ₂	0.96	0.06	4.6 ± 0.9

(211) (110), (101), (211) and 20% of rutile phase with 2θ : 27.4°, 36.1° and 54.4° corresponding to the planes (110), (101), (211)^{6,16}. However, it was not observed the presence of Cu⁰ and Au⁰ having a face-centered cubic structure (fcc) where the diffracting planes are (111), (200), (220) which correspond to 2θ : 43.24°; 50.35°; 73.96° for Cu (#PDF 4-784) and 38.17°; 44.37°; 64.55° for Au (#PDF 4-836)¹⁷ nor the presence of copper oxide phases such as CuO or Cu₂O¹⁸. This could be due to the low content of these metals or to the average diameter of the crystallites (< 5 nm) resulting in low intensity and broad peaks that in the presence of well-defined and high intensity crystalline peaks of TiO₂ support make their identification difficult¹⁹.

The transmission electron micrographs of Cu/TiO₂, Au/TiO₂ and AuCu/TiO₂ catalysts are shown in Figure 2.

For Cu/TiO₂ catalyst (Figure 2a) it was not observed in the TEM micrographs the presence of black dots while

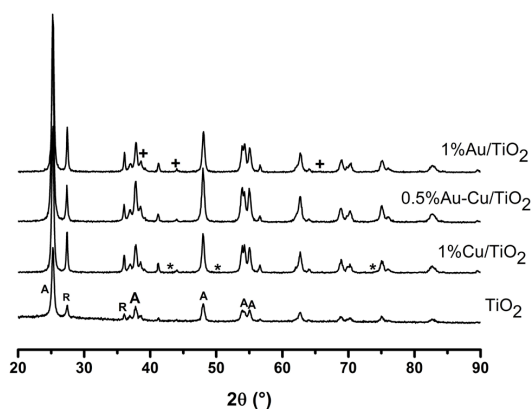


Figure 1. X-ray diffractograms of the TiO₂ support and the catalysts (A = peaks of Anatase phase, R = peaks of Rutile phase, * peaks position of Cu (fcc) phase and + peaks position of Au (fcc) phase)

for catalysts having Au (Figure 2b-d) they were observed having average sizes in the range of 3-5 nm (see Table 1). Figure 3 shows a high-angle annular dark-field scanning transmission electron microscopy (HAADF/STEM) image, EDS mapping and line-scan of Au_{0.50}Cu_{0.50}/TiO₂ catalyst.

HAADF/STEM image showed bright dots of small sizes (average 3 nm) what is coming from the differences between metals and support element atomic numbers contributing to a high contrast in the image showing that metal nanoparticles are dispersed on TiO₂ support. The EDS mapping and line scan confirmed that Au is exclusively located in the position of bright dots while Cu is also located at these positions in close contact with Au and distributed over the TiO₂ surface.

The temperature programmed reduction (TPR) profiles of TiO₂ support and Au/TiO₂, Cu/TiO₂ and Au_{0.50}Cu_{0.50}/TiO₂ catalysts are shown in Figure 4.

The H₂-TPR profile of the TiO₂-P25 support showed no reduction peaks in the studied temperature range as already reported in the literature for temperatures from ambient to 800 °C²⁰. The H₂-TPR profile of Cu/TiO₂ catalysts showed an intense peak at about 150 °C attributed to the reduction of CuO to Cu(0)²⁰⁻²³ and a small peak at about 375 °C that could be ascribed to the reduction of CuO nanoparticles having little or no interaction with the support^{23,24}. It was also observed on H₂-TPR profile of Cu/TiO₂ catalyst a peak at about 575 °C. Ramírez and Gutiérrez-Alejandre²⁵ observed a peak at about 570 °C in the TPR profile of pure anatase TiO₂ support. Kang et al.²² reported for CuO supported on pure anatase TiO₂ phase two peaks at 140 and 470 °C that were attributed to reduction of Cu⁺² to Cu⁰ and to the reduction of anatase phase, respectively; however, for CuO supported on pure rutile TiO₂ phase only one peak at around 120 °C was observed. Zhang et al.²⁶ described that no peaks were observed between 25 and 500 °C in the TPR profile of an anatase TiO₂ support; on the other hand, the TPR profile of the Pt/TiO₂ catalyst showed two peaks at 80 and 360 °C that were

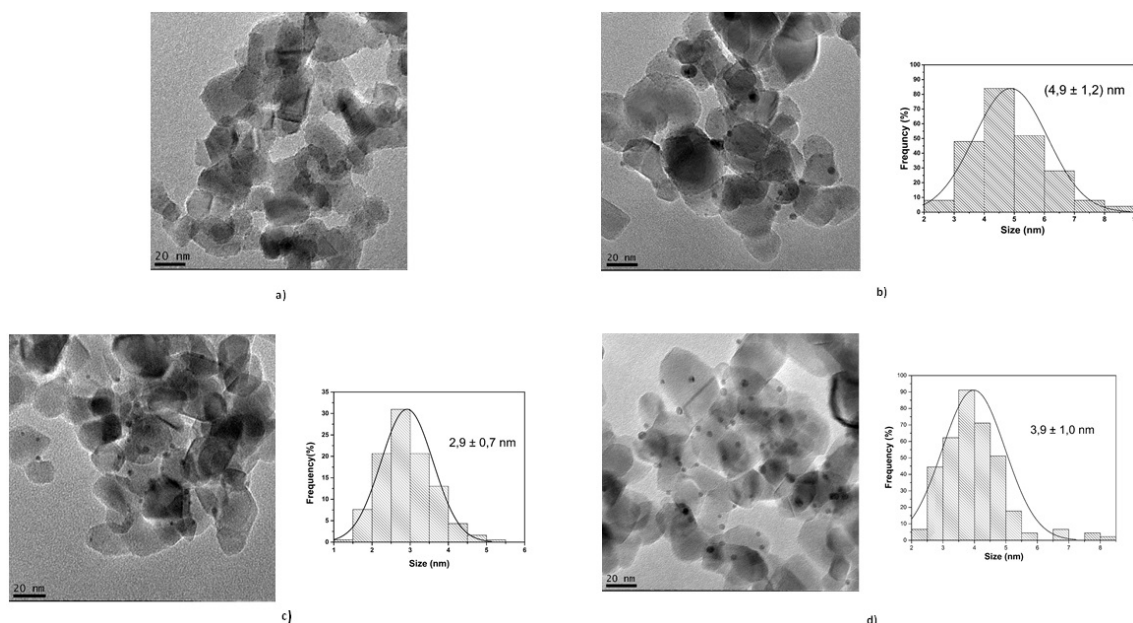


Figure 2. Transmission electron micrographs and histograms of a) Cu/TiO₂, b) Au/TiO₂, c) Au_{0.50}Cu_{0.50}/TiO₂ and d) Au_{0.75}Cu_{0.25}/TiO₂ catalysts

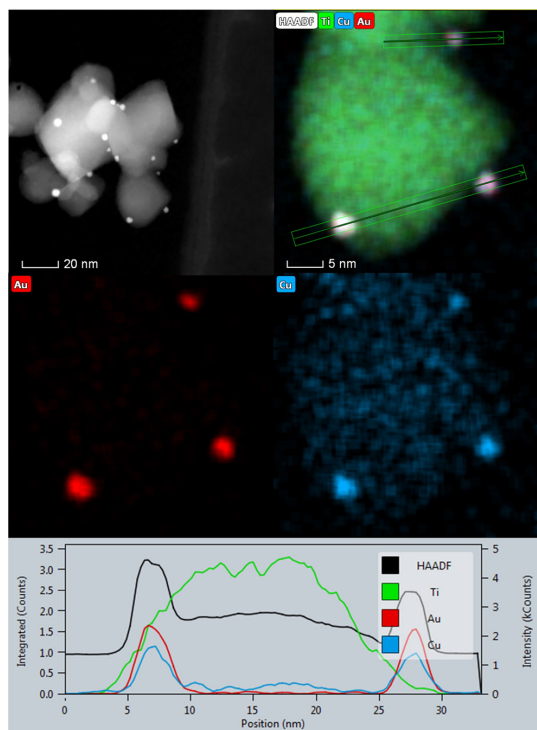


Figure 3. High-angle annular dark-field scanning transmission electron microscopy (HAADF/STEM) image, EDS mapping and line-scan of $\text{Au}_{0.50}\text{Cu}_{0.50}/\text{TiO}_2$ catalyst

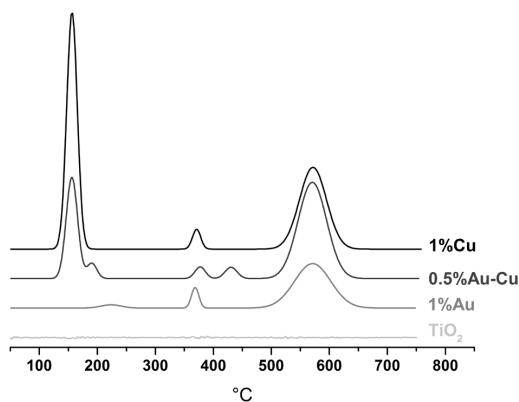


Figure 4. H_2 -TPR profiles of TiO_2 support and the catalysts

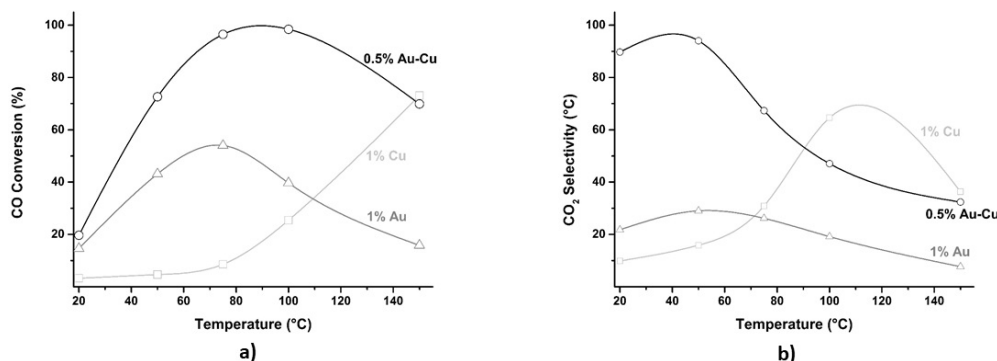


Figure 5. (a) CO conversion and (b) CO_2 selectivity in function of the temperature for Cu/TiO_2 , Au/TiO_2 and $\text{Au}_{0.50}\text{Cu}_{0.50}/\text{TiO}_2$ (1.0% CO , 1.0% O_2 , 98.0% H_2 and a space velocity of $15000 \text{ mL g}_{\text{cat}}^{-1} \text{ h}^{-1}$)

attributed to the reduction of PtO_x to metallic Pt and to the reduction of the surface capping oxygen of TiO_2 , respectively. Thus, the peak observed at $575 \text{ }^\circ\text{C}$ in the TPR profile may result from the reduction of the surface oxygen of anatase phase of TiO_2 P-25 support that is favored by the interaction with Cu species. The H_2 -TPR profile of Au/TiO_2 catalyst did not show reduction peaks below $100 \text{ }^\circ\text{C}$ suggesting that Au was predominantly found in the metallic form²⁷ taking into account that pre-treated (reduced) Au catalyst do not show any peak of reduction²⁸. However, it was observed a very small and broad peak at about $225 \text{ }^\circ\text{C}$ that could be related to ionic Au-species interacting with TiO_2 phase^{27,28}. For $\text{Au}_{0.50}\text{Cu}_{0.50}/\text{TiO}_2$ catalyst it was observed a peak at about $150 \text{ }^\circ\text{C}$ attributed to the reduction of CuO to $\text{Cu}(0)$ and a small and broad peak at about $180 \text{ }^\circ\text{C}$ that could be due to ionic Au-species interacting with CuO and TiO_2 phases. In the region of temperature between 350 and $450 \text{ }^\circ\text{C}$ two small peaks are observed for $\text{Au}_{0.50}\text{Cu}_{0.50}/\text{TiO}_2$ catalyst, which could be a result of the interaction of Au and Cu species with TiO_2 support and a peak at about $575 \text{ }^\circ\text{C}$ resulting from reduction of TiO_2 support. Thus, it could be inferred from these results that AuCu/TiO_2 catalysts prepared by this methodology exhibit most of the Au in metallic form while most of the Cu is in oxide form (CuO). In fact, by analyzing the results of H_2 -TPR and microscopy it could be inferred that Au and CuO_x species interact with each other and with TiO_2 support.

The catalytic performances of the Cu/TiO_2 , Au/TiO_2 and $\text{Au}_{0.50}\text{Cu}_{0.50}/\text{TiO}_2$ catalysts were studied in the temperature range of $20 \text{ }^\circ\text{C}$ to $150 \text{ }^\circ\text{C}$ (Figure 5). No previous treatments were done in these samples before catalytic tests and the results shown correspond to the second cycle of the catalytic reactions.

Cu/TiO_2 catalyst showed low CO conversions (below 20%) until $100 \text{ }^\circ\text{C}$ increasing to 75% at $150 \text{ }^\circ\text{C}$. The CO_2 selectivity showed a maximum value of 70% at around $120 \text{ }^\circ\text{C}$. Au/TiO_2 catalyst showed a maximum CO conversion of 55% at $75 \text{ }^\circ\text{C}$; however, CO_2 selectivity values were very low (around 20%) in all range of temperature. For all AuCu/TiO_2 catalysts prepared with different contents of Au and Cu the maximum CO conversions occurred at $100 \text{ }^\circ\text{C}$. In addition, the CO conversion values increased with the increase of Au content reaching a maximum value of 98.4% for $\text{Au}_{0.50}\text{Cu}_{0.50}/\text{TiO}_2$ catalyst (Figure 5a)

and, after that, these values began to decrease (92.0% for Au_{0.75}Cu_{0.25}/TiO₂ catalyst) as the amount of Au was increased further. Conversely, CO₂ selectivity values increased with the increase of Cu content and the values varied between 35% and 55% at 100 °C. The CO₂ selectivity value for Au_{0.50}Cu_{0.50}/TiO₂ catalyst was 47% (Figure 5b) reaching a maximum value of 55% for Au_{0.25}Cu_{0.75}/TiO₂ catalyst and after that decreased to 50% for Au_{0.10}Cu_{0.90}/TiO₂ catalyst. Thus, AuCu/TiO₂ catalysts showed to be more active for CO-PROX reaction than Au/TiO₂ and Cu/TiO₂ catalysts in the temperature range of 20 °C to 100 °C, as already observed for CO-PROX reaction¹³ and for CO-oxidation at low temperature¹⁴.

Figure 6 shows the CO conversion as a function of Au content (wt%) and nanoparticle sizes for AuCu/TiO₂ catalysts prepared with different contents of Au and Cu. It could be seen that there is a relationship between Au content and nanoparticles sizes where the maximum CO conversion was observed for the sample Au_{0.50}Cu_{0.50}/TiO₂ with similar quantities of Au and Cu and that's where a smaller size of the Au nanoparticles was observed.

The long-term stability test results for Au_{0.50}Cu_{0.50}/TiO₂ catalyst is shown in Figure 7 showing CO conversions above 90%

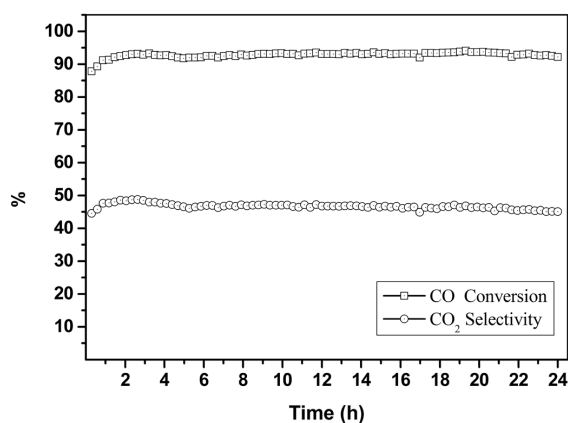


Figure 6. CO conversion at 100 °C in the function of Au content (wt%) and nanoparticle sizes for AuCu/TiO₂ catalysts with different Au and Cu content (1.0% CO, 1.0% O₂, 98.0% H₂, 100 °C and a space velocity of 15000 mL g_{cat}⁻¹ h⁻¹)

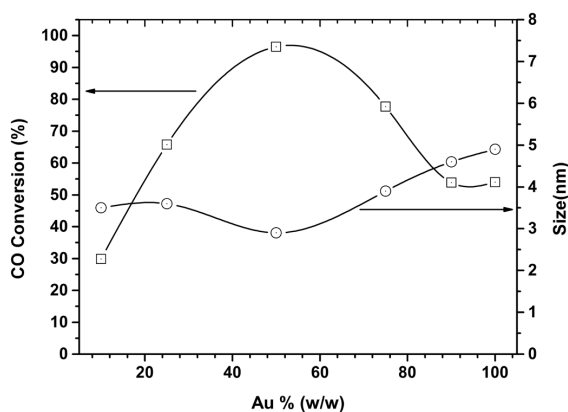


Figure 7. CO conversion and CO₂ selectivity in function of time for Au_{0.50}Cu_{0.50}/TiO₂ catalyst at 100 °C (1% of CO, 1% of O₂ and 98% of H₂, spatial velocity of 15000 mL g_{cat}⁻¹ h⁻¹)

and CO₂ selectivity values in the range of 45-50%, which remained stable throughout the period evaluated showing the stability of the catalysts under the applied reaction conditions. Similar results were observed by Sangeetha et al.¹³ in long test time using as catalyst Au/CuO_x-TiO₂ (1wt% of Au and a CuO_x:TiO₂ ratio of 4.8:95.2) at 80 °C for 49 h. A maximum CO conversion of 95% with a CO₂ selectivity of about 65% was obtained using a gas composition of 1.33% CO, 1.33% O₂, 65.33% H₂, and 32.01% He and a space velocity of 30000 mL g_{cat}⁻¹ h⁻¹.

Sangeetha et al.¹³ also observed an increase of maximum CO conversion and CO₂ selectivity for CO-PROX reaction comparing Au/TiO₂ and Au/CuO_x-TiO₂ catalysts and attributed this increase due to the presence of Au(0) and CuO_x species, where CuO_x-TiO₂ was proposed to be a supplier or storage of oxygen. Wang et al.²⁹ studied the synergistic effects of different Au bimetallic alloy catalysts in low temperature CO oxidation and observed for AuCu alloy catalyst that a phase segregation occurs during CO oxidation forming a Au@CuO_x hybrid structure (nano or even sub-nano CuO_x supported on Au nanoparticles) resulting in interfacial sites between them. FTIR studies of CO adsorption showed that CO adsorbed on Au(0) while CuO_x species were responsible for providing active oxygen in the same way as reducible oxides do. Recently it was shown that CuO not Cu₂O species played a more critical role for CO oxidation at low temperature and that CuO and Au(0) species enhanced the activity of Au/CuO catalyst only if a strong interaction occurs between them¹⁵.

4. Conclusions

Active, selective and stable AuCu/TiO₂ catalysts was prepared by a simple one-step methodology for CO-PROX reaction. The AuCu/TiO₂ catalysts exhibited good activities and selective in the range of 75-100 °C and presented a better catalytic activity when compared to the monometallic ones. The analyses showed that Au is predominantly found in its metallic form while Cu in its oxide form and that Au(0) and CuO_x species are in good interaction with each other and with TiO₂ support.

5. Acknowledgments

The authors gratefully acknowledge support from FAPESP and SHELL Brasil through the 'Research Centre for Gas Innovation – RCGI' (FAPESP Proc. 2014/50279-4), hosted by the University of São Paulo, and the support given by ANP (Brazil's National Oil, Natural Gas and Biofuels Agency) through the R&D levy regulation. FAPESP / Shell Proc. n° 2017/11937-4 (CINE); FAPESP Proc. n° 2014/09087-4, and CNPq Proc. n° 304869/2016-3 are grateful for financial support. Centro de Ciência e Tecnologia dos Materiais (CCTM) – IPEN-CNEN/SP and LNNano-CNPEM (JEOL JEM 2100F) are greatly acknowledged for the use of TEM facilities.

6. References

- Mishra A, Prasad R. Review on preferential oxidation of carbon monoxide in hydrogen rich gases. Bull Chem React Eng Catal. 2011;6(1):1-14. <http://dx.doi.org/10.9767/bcrec.6.1.191.1-14>.

2. Liu K, Wang A, Zhang T. Recent advances in preferential oxidation of CO reaction over Platinum Group Metal Catalysts. *ACS Catal.* 2012;2(6):1165-78. <http://dx.doi.org/10.1021/cs200418w>.
3. Huang S, Hara K, Fukuoka A. Green catalysis for selective CO oxidation in hydrogen for fuel cell. *Energy Environ Sci.* 2009;2(10):1060-8. <http://dx.doi.org/10.1039/b910696k>.
4. Park ED, Lee D, Lee HC. Recent progress in selective CO removal in a H₂-rich stream. *Catal Today.* 2009;139(4):280-90. <http://dx.doi.org/10.1016/j.cattod.2008.06.027>.
5. Saavedra J, Whittaker T, Chen Z, Pursell CJ, Rioux RM, Chandler BD. Controlling activity and selectivity using water in the Au-catalysed preferential oxidation of CO in H₂. *Nat Chem.* 2016;8(6):584-9. <http://dx.doi.org/10.1038/nchem.2494>.
6. Leal GB, Ciotti L, Watacabe BN, Loureiro da Silva DC, Antoniassi RM, Silva JCM, et al. Preparation of Au/TiO₂ by a facile method at room temperature for the CO preferential oxidation reaction. *Catal Commun.* 2018;116:38-42. <http://dx.doi.org/10.1016/j.catcom.2018.07.021>.
7. Klyushin AY, Jones TE, Lunkenbein T, Kube P, Li X, Havecker M, et al. Strong metal support interaction as a key factor of Au activation in CO oxidation. *ChemCatChem.* 2018;10(18):3985-9. <http://dx.doi.org/10.1002/cctc.201800972>.
8. Panayotov DA, Morris JR. Surface chemistry of Au/TiO₂: thermally and photolytically activated reactions. *Surf Sci Rep.* 2016;71(1):77-271. <http://dx.doi.org/10.1016/j.surfrep.2016.01.002>.
9. Wang Y, Widmann D, Behm RJ. Influence of TiO₂ bulk defects on CO adsorption and CO oxidation on Au/TiO₂: electronic metal-support interactions (EMSI) in supported Au catalysts. *ACS Catal.* 2017;7(4):2339-45. <http://dx.doi.org/10.1021/acscatal.7b00251>.
10. Lakshmanan P, Park JE, Park ED. Recent advances in preferential oxidation of CO in H₂ over gold catalysts. *Catal Surv Asia.* 2014;18(2-3):75-8. <http://dx.doi.org/10.1007/s10563-014-9167-x>.
11. Qiao B, Liu J, Wang Y-G, Lin Q, Liu X, Wang A, et al. Highly efficient catalysis of preferential oxidation of CO in H₂-rich stream by gold single-atom catalysts. *ACS Catal.* 2015;5(11):6249-54. <http://dx.doi.org/10.1021/acscatal.5b01114>.
12. Tabakova T. Recent advances in design of gold-based catalysts for H₂ clean-up reaction. *Front Chem.* 2019;7:517. <http://dx.doi.org/10.3389/fchem.2019.00517>.
13. Sangeetha P, Zhao B, Chen Y-W. Au/CuO_x-TiO₂ catalysts for preferential oxidation of CO in hydrogen stream. *Ind Eng Chem.* 2010;49(5):2096-102. <http://dx.doi.org/10.1021/ie901233e>.
14. Duh FC, Lee DS, Chen YW. Au/CuO_x-TiO₂ catalysts for CO oxidation at low temperature. *Modern Research in Catalysis.* 2013;02(01):1-8. <http://dx.doi.org/10.4236/mrc.2013.21001>.
15. Qi C, Zheng Y, Lin H, Su H, Sun X, Sun L. CO oxidation over gold catalysts supported on CuO/Cu₂O both in O₂-rich and H₂-rich streams: necessity of copper oxide. *Appl Catal B.* 2019;253:160-9. <http://dx.doi.org/10.1016/j.apcatb.2019.03.081>.
16. Jiang X, Manawan M, Feng T, Qian R, Zhao T, Zhou G, et al. Anatase and rutile in evonik aerioxide P25: heterojunctioned or individual nanoparticles? *Catal Today.* 2018;300:12-7. <http://dx.doi.org/10.1016/j.cattod.2017.06.010>.
17. Zhao D, Xiong X, Qu C-L, Zhang N. Remarkable enhancement in Au catalytic utilization for liquid redox reactions by galvanic deposition of Au on Cu nanoparticles. *J Phys Chem C.* 2014;118(33):19007-16. <http://dx.doi.org/10.1021/jp500908e>.
18. Choi D, Jang D-J. Facile fabrication of CuO/Cu₂O composites with high catalytic performances. *New J Chem.* 2017;41(8):2964-72. <http://dx.doi.org/10.1039/C6NJ03949A>.
19. Yang Y-F, Sangeetha P, Chen Y-W. Au/TiO₂ catalysts prepared by photo-deposition method for selective CO oxidation in H₂ stream. *Int J Hydrogen Energy.* 2009;34(21):8912-20. <http://dx.doi.org/10.1016/j.ijhydene.2009.08.087>.
20. Li J, Lu G, Wu G, Mao D, Guo Y, Wang Y, et al. Effect of TiO₂ crystal structure on the catalytic performance of Co₃O₄/TiO₂ catalyst for low-temperature CO oxidation. *Catal Sci Technol.* 2014;4(5):1268-75. <http://dx.doi.org/10.1039/C3CY01004J>.
21. Li K, Wang Y, Wang S, Zhu B, Zhang S, Huang W, et al. A comparative study of CuO/TiO₂-SnO₂, CuO/TiO₂ and CuO/SnO₂ catalysts for low-temperature CO oxidation. *J Nat Gas Chem.* 2009;18(4):449-52. [http://dx.doi.org/10.1016/S1003-9953\(08\)60144-9](http://dx.doi.org/10.1016/S1003-9953(08)60144-9).
22. Kang MY, Yun HJ, Yu S, Kim W, Kim ND, Yi J. Effect of TiO₂ crystalline phase on CO oxidation over CuO catalysts supported on TiO₂. *J Mol Catal Chem.* 2013;368-369:72-7. <http://dx.doi.org/10.1016/j.molcata.2012.11.021>.
23. Oros-Ruiz S, Zanella R, Prado B. Photocatalytic degradation of trimethoprim by metallic nanoparticles supported on TiO₂-P25. *J Hazard Mater.* 2013;263:28-35. <http://dx.doi.org/10.1016/j.jhazmat.2013.04.010>.
24. Bocuzzi F, Chiorino A, Martra G, Gargano M, Ravasio N, Carrozzini B. Preparation, characterization and activity of Cu/TiO₂ catalysts. *J Catal.* 1997;165:120-39.
25. Ramírez J, Gutiérrez-Alejandre A. Relationship between hydrodesulfurization activity and morphological and structural changes in NiW hydrotreating catalysts supported on Al₂O₃-TiO₂ mixed oxides. *Catal Today.* 1998;43(1-2):123-33. [http://dx.doi.org/10.1016/S0920-5861\(98\)00141-2](http://dx.doi.org/10.1016/S0920-5861(98)00141-2).
26. Zhang C, He H, Tanaka K. Catalytic performance and mechanism of a Pt/TiO₂ catalyst for the oxidation of formaldehyde at room temperature. *Appl Catal B.* 2006;65(1-2):37-43. <http://dx.doi.org/10.1016/j.apcatb.2005.12.010>.
27. Pérez P, Soria MA, Carabineiro SAC, Maldonado-Hodar FJ, Mendes A, Madeira LM. Application of Au/TiO₂ catalysts in the low-temperature water-gas shift reaction. *Int J Hydrogen Energy.* 2016;41(8):4670-81. <http://dx.doi.org/10.1016/j.ijhydene.2016.01.037>.
28. Magadzu T, Yang JH, Hena JD, Kung MC, Kung HH, Scurrell MS. Low temperature water-gas shift reaction over Au-supported on anatase in the presence of copper: EXAFS/XANES analysis of gold-copper ion mixtures on TiO₂. *J Phys Chem C.* 2017;121(16):8812-23. <http://dx.doi.org/10.1021/acs.jpcc.6b11419>.
29. Wang A, Liu XY, Mou CY, Zhang T. Understanding the synergistic effects of gold bimetallic catalysts. *J Catal.* 2013;308:258-71. <http://dx.doi.org/10.1016/j.jcat.2013.08.023>.